Journal of Materials Chemistry A

Accepted Manuscript

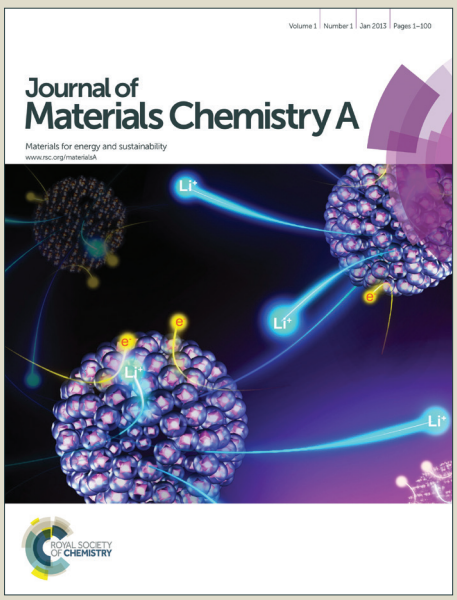

ROYAL SOCIETY OF CHEMISTRY

www.rsc.org/materialsA

Table of contents entry

Picolinic acid anchored dye JA2 onto the TiO_2 via tridentate mode, the JA2+TTR2 based-device showed the highest PCE of 8.98%.

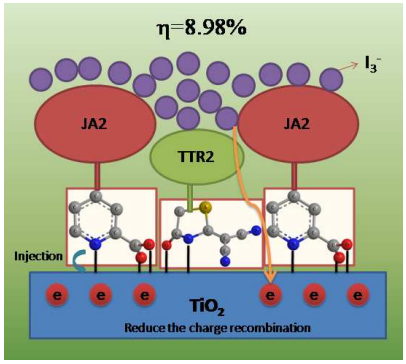

Cite this: DOI: 10.1039/c0xx00000x

www.rsc.org/xxxxxx

ARTICLE TYPE

Picolinic Acid as An Efficient Tridentate Anchoring Group Adsorbing at Lewis acid sites and Brønsted acid sites of TiO_2 Surface in Dye-Sensitized Solar Cells

Hai-Lang Jia,[a] Ming-Dao Zhang,[a] Ze-Min Ju,[a] He-Gen Zheng*[a] and Xue-Hai Ju*[b]

Received (in XXX, XXX) Xth XXXXXXXXX 20XX, Accepted Xth XXXXXXXXX 20XX
DOI: 10.1039/b000000x

We developed a novel efficient tridentate anchoring group which can anchor dye onto the TiO_2 surface via synchronously choosing Lewis acid sites and Brønsted acid sites of the TiO_2. With the purpose of comparing the traditional carboxylate anchoring group to picolinic acid, two new D-π-A porphyrin dyes (JA1 and JA2) differing only in anchoring groups have been synthesized and applied to the dye-sensitized solar cells. The picolinic acid as an anchoring group in the dye JA2 not only extended the scope of the spectral response, but also improved the charge transport properties and enhanced the electron injection efficiency. The PCE of JA1 based-device (carboxylate as the anchoring group) was 5.76%. The PCE of JA2 based-device was 7.20%, which increased by 25% compared with JA1. The dye TTR2 was used as a cosensitizer, it would not just make up for the poor absorption of porphyrin dyes in the 470-550 nm range, and would suppress the main dyes aggregation and reduce the charge recombination rate. We found that picolinic acid anchor was more suitable for cosensitization system than carboxylate anchor, for there was almost no competitive adsorption between JA2 and TTR2. The JA2+TTR2 based-device showed the highest PCE of 8.98% under AM 1.5G irradiation.

1. Introduction

As the world oil resource drying up, the development and utilization of new energy has become more and more urgent. Dye-sensitized solar cells (DSSCs) as a promising photovoltaic technology have received widespread attention,[1-3] due to their low costs and high photoelectric conversion efficiency. The DSSC is composed of photoanode, sensitizers, redox electrolyte and counter electrode.[4-6] After more than 20 years development, a variety of efficient sensitizer has been successfully synthesized, including ruthenium-complexes, zinc-porphyrins and organic dyes.[7-12] Recently, Grätzel and co-workers prepared porphyrin dye SM315, which showed the highest PCE of 13% with the cobalt-based redox electrolyte.[13]

In general, both the metal-complex sensitizers and organic sensitizers were often designed a typical donor-π-acceptor (D-π-A) framework,[14-16] due to their efficient intra-molecular charge transfer (ICT) properties. Researchers have developed many kinds of outstanding donors, such as triarylamine, diphenylamine, tetrahydroquinoline, phenothiazine, indoline and coumarin.[17-20] In DSSCs, the choice of suitable anchoring group was very important. The anchoring group determined the electron injection rate and the binding energy of the dye on semiconductor surface. However, the research about the anchoring group was not enough. To date, the efficient anchoring group was just the carboxylate.[1,7,13,21] In recent years, some new anchoring groups have been developed, such as pyridine,[22] phosphate,[23] hydroxamate[24,25] and catechol.[26] Thus, the development of new efficient anchoring group is very necessary. Carboxylate is often used as an anchoring group in DSSC, for its good electronic coupling on the dye-TiO_2 interface and high electron injection efficiency. However, the carboxylate anchoring group also has shortcomings. For example, some dyes with carboxylate anchoring groups often detached from the TiO_2 surface when cosensitized with the cosensitizer.[27] If the adsorbed amounts of the main dye molecules was reduced, the performance of the device would be decreased.[28] One of the main reasons is that there is competitive adsorption between the main dye and the cosensitizer.[29,30] Because the carboxylate anchoring group is vulnerable to degradation, even under the condition of trace quantities of water. Therefore, the anchoring group has a significant impact on the cosensitization system. Many reports have shown that the cosensitization system can improve the performance of the DSSC, for it can not only extend the absorption spectrum, but also prevent charge recombination, so as to improve the short-circuit current density (J_{sc}) and the open-circuit photovoltage (V_{oc}) of DSSCs.[31,32] For example, cosensitization of zinc porphyrin dye YD2-*o*-C8 with organic dye Y123 greatly improved the performance of the device, showing a high PCE of 12.3% under AM 1.5G irradiation.[33] But the competitive adsorption problem has not been solved, so we need to develop a new anchoring group to solve it. Fortunately, we found that the picolinic acid can be used as a promising anchoring group, which not only can anchor the dye onto the

TiO_2 surface more firmly, but also can enhance the electron injection rate via tridentate mode.

Among the efficient sensitizers, zinc-porphyrin has typical absorption at the Soret bands (400-450 nm) and the Q bands (550-650 nm).[34-38] In this paper, we synthesized two typical D-π-A porphyrin dyes JA1 and JA2. We used carboxylate and picolinic acid as the anchoring group, respectively. Remarkably, the J_{sc}, V_{oc} and PCE values of JA1and JA2 have a big difference in the photovoltaic performance test. We choose picolinic acid as the anchoring group, it can extend the scope of the spectral response of dye JA2. Even more important, it synchronously choosing Lewis acid sites and Brønsted acid sites of TiO_2 when dye JA2 was adsorbed on the TiO_2 surface. Thus, the picolinic acid can anchor dye JA2 onto the TiO_2 surface more firmly and can improve the electronic coupling on the dye-TiO_2 surface.[22] In addition, we adopt phenothiazine as the electron donor, and introduced long alkyl chain onto the donor to suppress dye aggregation.[39-41] Moreover, we used dye TTR2 as the cosensitizer, whose maximum absorption peak lies at 521 nm.[42] This is a good way to make up for the poor absorption of zinc-porphyrin dye in the 470-550 nm range. The dye TTR2 can occupy the voids between the main dye molecules. Thus, this way can prevent the I_3^- of the electrolyte penetrating into the TiO_2 surface, thereby reducing the charge recombination.[28,43,44] Cosensitization of JA1 and TTR2 showed the PCE of 6.75%, and cosensitization of JA2 and TTR2 showed the highest PCE of 8.98%. The results indicate that the picolinic acid can be as a promising anchoring group to improve the performance of DSSC.

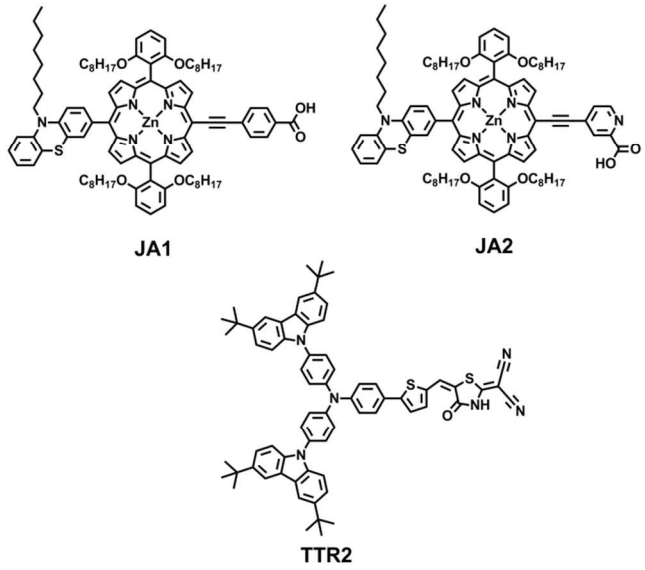

Scheme 1. Chemical structures of **JA1**, **JA2** and cosensitizer **TTR2**.

2. Results and Discussion

Synthesis and Characterizations

The chemical structures of JA1, JA2 and TTR2 were shown in Scheme 1, and the synthetic routes were depicted in Scheme S1. We further characterize the photophysical and electrochemical properties, and the photovoltaic performance of these dyes.

Optical Properties

Table 1 Optical and electrochemical properties of dyes

Dye	[a] λ_{max}/nm ($\varepsilon\times10^5$ M^{-1} cm^{-1})	[b] λ_{max}/nm	[c] E_{OX} /V (vs. NHE)	[d] $E_{0\text{-}0}$/eV	[e] E^*_{OX} /V (vs. NHE)
JA1	442(3.03), 566(0.16), 616(0.25)	638	0.88	2.01	-1.13
JA2	447(3.09), 568(0.21), 622(0.40)	646	0.94	2.00	-1.06

[a] Absorption maximum in DCM solution (1×10^{-5} M), [b] emission maximum in DCM solution (1×10^{-5} M), [c] the ground state oxidation potentials, [d] $E_{0\text{-}0}$ was estimated from the intercept of the normalized absorption and emission spectra, [e] E^*_{OX} was calculated by the formula: $E^*_{OX} = E_{OX} - E_{0\text{-}0}$.

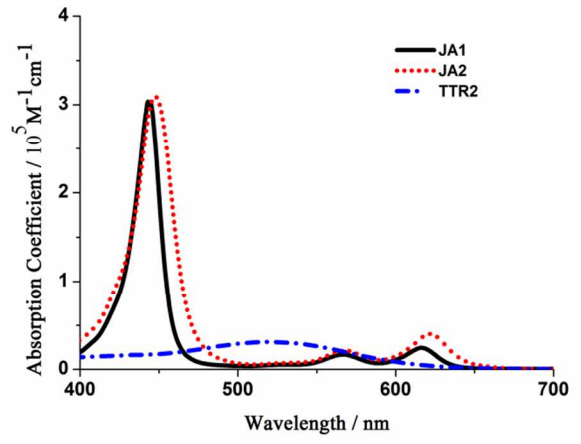

Fig. 1 UV-Vis absorption spectra of **JA1**, **JA2** and **TTR2** in DCM.

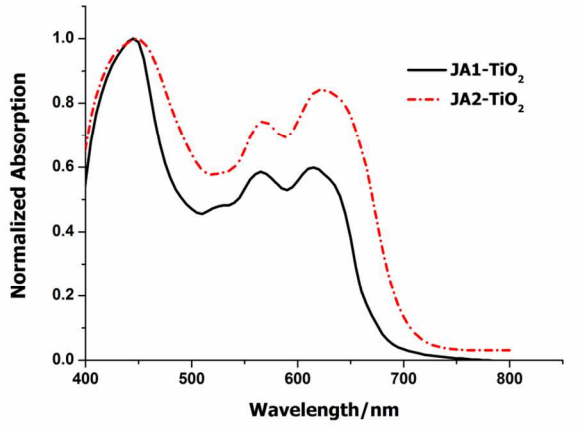

Fig. 2 Absorption spectra of the dyes anchored on the 14 μm porous TiO_2 nanoparticle films.

The UV-Vis absorption spectra of JA1, JA2 and TTR2 in DCM were shown in Fig. 1, and the corresponding data were listed in Table 1. The dyes JA1 and JA2 exhibited typical porphyrin absorption characteristics. Obviously, the absorption spectrum of dye JA2 was red-shifted compared with JA1, which may be due to its better intramolecular charge transfer properties. The absorption spectra of JA1 and JA2 showed intense Soret bands at 442 nm and 447 nm, respectively, and they had almost the same

molar extinction coefficient. The absorption spectrum of JA2 at Q bands displayed significant enhancement compared to JA1, the maximum absorption peak was red-shifted by 6 nm from 616 to 622 nm, and the molar extinction coefficient of JA2 (4.0×10^4 M^{-1} cm^{-1}) was 1.60 times than that of JA1 (2.5×10^4 M^{-1} cm^{-1}). We further investigate their emission spectra (Fig. S1), their maximum peaks lie at 638 and 646 nm, respectively. It is consistent with the trend of the absorption spectra of the two dyes. It is clear that the two dyes show weak absorption in the 470-550 nm range, whereas the maximum absorption peak of TTR2 lies at 521 nm. The results indicate that the dye TTR2 can compensate well the weak absorption of the two dyes in the 470-550 nm range. Fig. 2 showed the UV-Vis absorption spectra of JA1 and JA2 adsorbed onto 14 μm thick TiO_2 films. The absorption ranges of the two dyes were all broadened, especially for JA2, it displayed significant enhancement compared with JA1 at Q bands. The results will be beneficial to improve their light-harvesting ability.

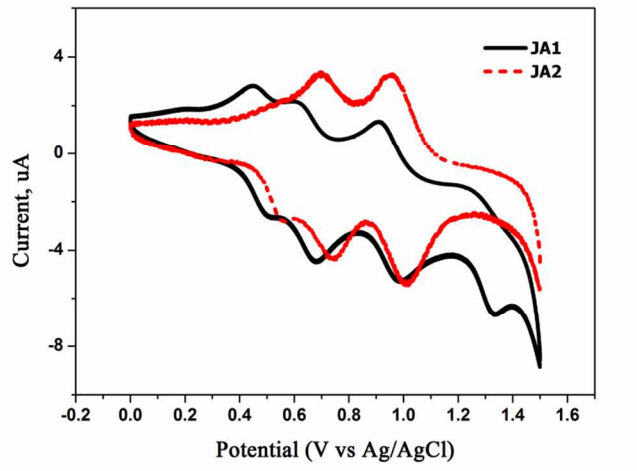

Fig. 3 Cyclic voltammogram of **JA1** and **JA2** in DCM (0.1 M $TBAPF_6$, glassy carbon electrode as working electrode, Pt as counter electrode, Ag/Ag^+ as reference electrode, scan rate: 100 mV s^{-1}), Potentials measured vs. ferrocene/ferrocenium (Fc/Fc^+) couple were converted to normal hydrogen electrode (NHE) by addition of +0.63 V.

Electrochemical Properties

The electrochemical characterization of JA1 and JA2 was investigated by cyclic voltammetry (Fig. 3), and corresponding data were collected in Table 1. The ground state oxidation potentials (E_{OX}) of JA1 and JA2 were both quasi-reversible, with values of +0.88 V and +0.94 V (versus NHE), respectively. The value of JA2 was higher than that of JA1 by 60 mV, it may be due to the stronger electronic withdrawing ability of picolinic acid. Nevertheless, they were both positive than the redox potential of the I^-/I_3^- couple (0.4 V versus NHE), guaranteeing efficient dye regeneration. The Zero-Zero transition energies ($E_{0\text{-}0}$) of JA1 and JA2 were 2.01 eV and 2.00 eV, respectively. They were estimated from the intercept of normalized UV-Vis absorption spectra and emission spectra. The excited oxidation potentials (E^*_{OX}) can be calculated by $E^*_{OX} = E_{OX} - E_{0\text{-}0}$. The corresponding E^*_{OX} of JA1 and JA2 were -1.13 V and -1.06 V, respectively. The values were both much more negative than the Fermi level of TiO_2 (-0.5 V versus NHE), insuring an efficient electron injection process from the excited dye into the conduction band of TiO_2.[45-47]

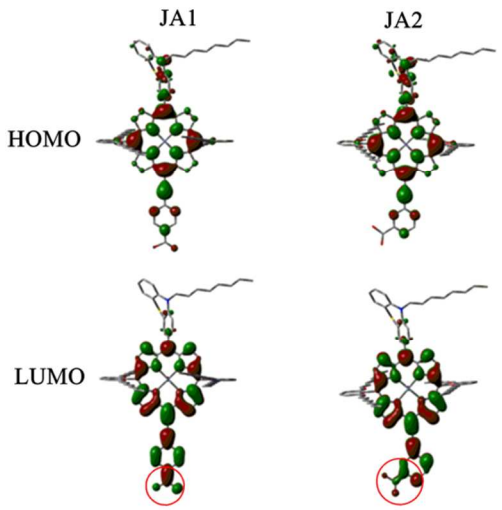

Fig. 4 The HOMO and LUMO frontier molecular orbitals of **JA1** and **JA2** calculated at the DFT-B3LYP/LanL2DZ level with the Gaussian 09 suite of programs.

Theoretical Calculations

To further insight into the electron distribution of the frontier orbitals of the two dyes, density functional theory (DFT) was performed at the DFT-B3LYP/LanL2DZ level with the Gaussian09 suite of programs. As shown in Fig. 4, it is obvious that the electron density of JA1 and JA2 for the HOMO was shared by the phenothiazine donor group and porphyrin ring, and the LUMO was essentially spread over the anchoring group and the porphyrin ring. The HOMO and LUMO of the two dyes displayed good overlap between the donor group and the anchoring group, which suggested that the photoinduced charge can be efficiently injected from the excited dye into the conduction band of TiO_2. In addition, from Table S1, we found that the contribution of carboxylate of JA1 to LUMO was 6%, whereas the contribution of picolinic acid of JA2 to LUMO was 19%. Obviously, the significant contribution of the picolinic acid to LUMO can provide better electronic coupling on the dye-TiO_2 surface, leading to more efficient electron injection.[23,48]

Fourier-transform Infrared Spectroscopy

The fourier-transform infrared spectroscopy (FTIR) of the dye powders and the dyes adsorbed on TiO_2 surface were shown in Fig. S2. For powder of dye JA1, the carbonyl stretch ν(C=O) was observed at 1687 cm^{-1}. After adsorbed onto the TiO_2 surface, the carbonyl stretch ν(C=O) disappeared. And a new band appeared at 1645 cm^{-1}, which represented the antisymmetric stretching $\nu(COO^-_{as})$.[13,44,49] The results indicate that JA1 adsorbed at the Brønsted acid sites of the TiO_2 surface via dehydration reactions. In addition, The carbonyl stretch ν(C=O) was observed at 1652 cm^{-1} for powder of dye JA2, and the stretching vibrations of C=C or C=N were observed at 1594 cm^{-1}, 1491 cm^{-1}, 1455 cm^{-1} and 1416 cm^{-1} for the dye powder. After adsorbed on the TiO_2 surface, the carbonyl stretch ν(C=O) disappeared, moreover, a new band appeared at 1615 cm^{-1}.[22,50] The results clearly indicate

that the dye JA2 was adsorbed on the TiO_2 surface not only by the carboxylate moiety at the Brønsted acid sites, but also adsorbed at the Lewis acid sites of the TiO_2 surface by the pyridine ring. Therefore, picolinic acid as an efficient tridentate anchoring group can improve the performance of the DSSCs.

Table 2 Fitting parameter (χ^2) and excited-state lifetime (τ_1, τ_2) from the time-resolved fluorescence experiments

Dye	χ^2	τ_1 (ns)	τ_2 (ns)
JA1-THF	1.105	1.96	8.14
JA1-TiO_2	1.236	0.49	2.69
JA2-THF	1.022	2.40	10.50
JA2-TiO_2	1.285	0.22	2.52

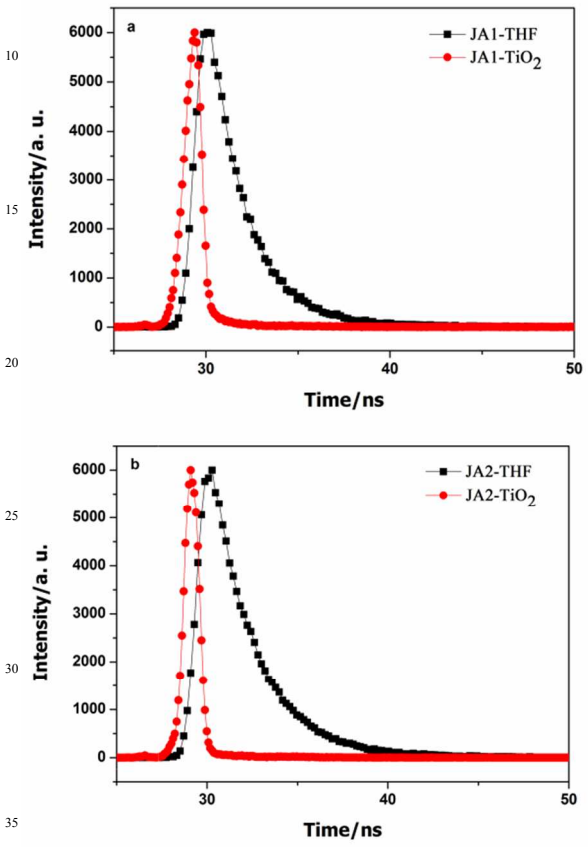

Fig. 5 Fluorescence decay curves of dyes in THF (black line) and dyes adsorbed onto the TiO_2 surface (red line).

Electron Injection Rate Analysis

The time-resolved fluorescence experiments were performed to study the differences in the electron injection process between the two dyes (Fig. 5), and corresponding data were collected in Table 2. In THF, the lifetime values of JA1 were 1.96 ns (τ_1) and 8.14 ns (τ_2), and the values of JA2 were 2.40 ns (τ_1) and 10.50 ns (τ_2). It is clear that the two excited dyes have enough time to complete the electron injection process. After adsorbed on the TiO_2 surface, the lifetime values of JA1 reduced to 0.49 ns (τ_1) and 2.69 ns (τ_2), and the values of JA2 reduced to 0.22 ns (τ_1) and 2.52 ns (τ_2). Considering the electron injection is the only way for the deactivation of excited dye, thus the excited charge transfer from JA2 to the conduction band of TiO_2 is more effective than that in case of JA1.[29,51]

Table 3 Photovoltaic parameters of the DSSCs obtained from the *J-V* curves

Dye	J_{sc} (mA cm^{-2})	V_{oc} (mV)	*FF* (%)	η (%)	Dye adsorbed amounts (10^{-8} mol cm^{-2})
[a] JA1	12.10	701	67.8	5.76	7.82
[a] JA2	15.02	719	66.7	7.20	6.80
[b] JA1+TTR2	13.42	732	68.6	6.75	4.63/4.67
[b] JA2+TTR2	17.75	755	67.0	8.98	6.77/1.65
[c] TTR2	10.97	762	68.0	5.71	

The size of the active area for each cell is 0.16 cm^2, [a] the DSSCs were measured under AM 1.5G irradiation, the photoanode was immersed in a solution of the porphyrin (0.2 mM) for 18 h, [b] the cosensitized DSSCs were measured under AM 1.5G irradiation, the photoanode was immersed in a solution of the porphyrin (0.2 mM) for 18 h and then immeresed in a solution of the TTR2 (0.3 mM) for 1.5 h, [c] reported in reference 42.

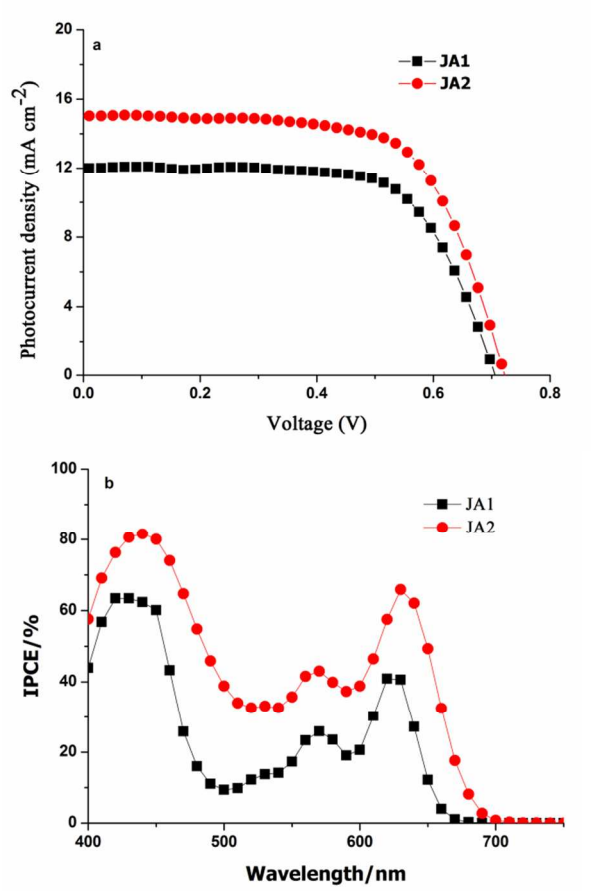

Fig. 6 (a) The *J-V* curves of DSSCs based on **JA1** and **JA2**. (b) The IPCE curves of DSSCs based on **JA1** and **JA2**.

Photovoltaic Performance of DSSCs

We performed the DSSCs experiments, the photovoltaic parameters were collected in Table 3, and the *J-V* curves of DSSCs were shown in Figure 6. The JA2 based-device showed a higher PCE of 7.20% compared with the JA1 (5.76%). The big difference between the PCE of the two DSSCs can be attributed to their different short-circuit current density (J_{sc}) and open-circuit photovoltage (V_{oc}). The V_{oc} of JA2 (719 mV) was higher

than that of JA1 (701 mV) by 18 mV, it is mainly due to the better charge transport properties of the JA2 based-device. In addition, we think that the picolinic acid as the anchoring group will make the dye molecules arrange to tilted orientation when adsorbed on the TiO_2 surface by the geometry optimization (Fig. S3). The result is helpful to reduce the charge recombination by preventing the I_3^- of the electrolyte penetrating into the TiO_2 surface. Thus, the adsorption amounts of JA2 (6.80×10^{-8} mol cm^{-2}) was lower than that of JA1 (7.82×10^{-8} mol cm^{-2}). Obviously, the J_{sc} of JA2 (15.02 mA cm^{-2}) was much larger than that of JA1 (12.10 mA cm^{-2}). It is consistent with the incident photon-to-current conversion efficiency (IPCE) of the DSSCs (Fig. 6b). The IPCE values of JA2 exceeded 70% from 410 to 465 nm, and attained 80.7% at 445 nm at Soret bands. Whereas, the values of JA1 were much lower than that of JA2 in this region, the maximum value of JA1 was only 62% at 440 nm at Soret bands. It is clear that the IPCE curve of JA1 was much lower and narrower than that of JA2 at Q bands. Compared with the UV-Vis absorption spectra, we knew that the dye JA2 had a better light-harvesting ability. Moreover, for dye JA2, the picolinic acid as an efficient tridentate anchoring group can choose the Lewis acid sites and Brønsted acid sites of TiO_2 surface synchronously, and it can anchor dye JA2 onto the TiO_2 surface more firmly and enhance the electron injection efficiency.

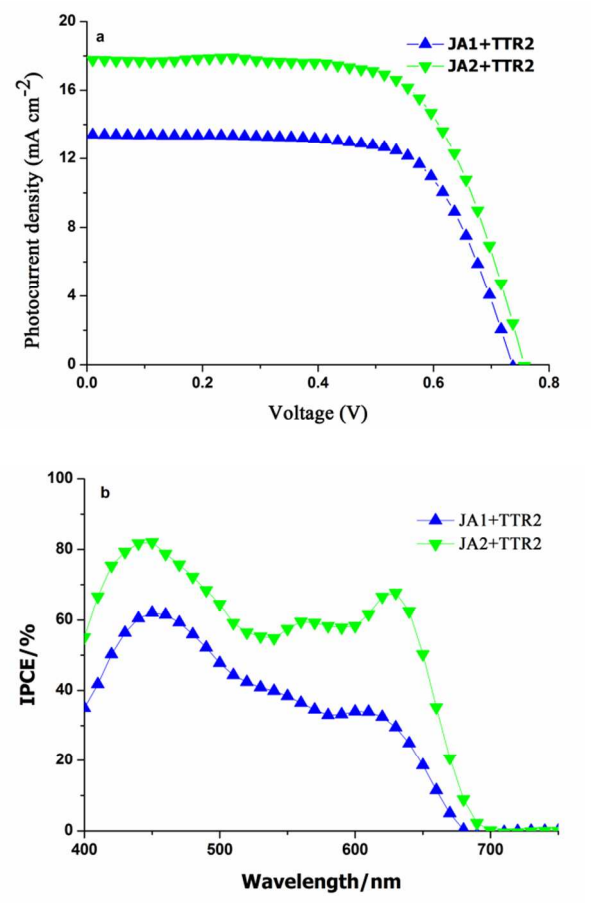

Fig. 7 (a) The *J-V* curves of DSSCs based on **JA1+TTR2** and **JA2+TTR2**. (b) The IPCE curves of DSSCs based on **JA1+TTR2** and **JA2+TTR2**.

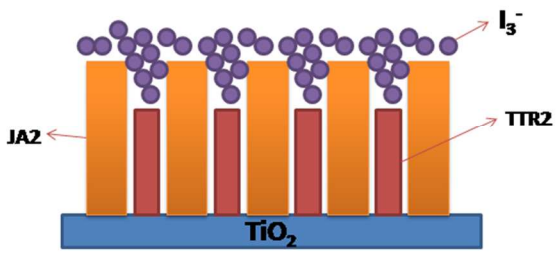

Fig. 8 The sketch map of adsorbed **JA2+TTR2** onto the TiO_2 surface.

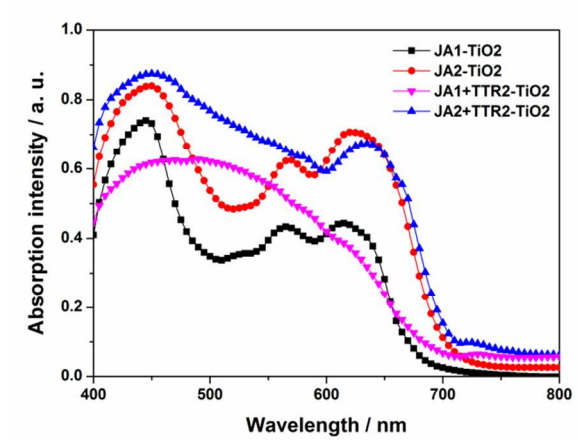

Fig. 9 Absorption spectra of the **JA1+TTR2** and **JA2+TTR2** anchored on the 14 μm porous TiO_2 nanoparticle films (cosensitized 1.5 h).

Cosensitization Systems

In order to improve the PCE of the DSSCs, we took the dye TTR2 as the cosensitizer. The corresponding photovoltaic parameters were collected in Table 3, and the *J-V* curves of DSSCs were shown in Fig. 7. After suitable screening of the cosensitization time (Table S2), it was found that the best cosensitization time was 1.5 h. The cosensitizer TTR2 showed the PCE of 5.71%, with a high V_{oc} (762 mV).[42] It has been known that the V_{oc} of the cosensitization system was intermediate in value between the main dye and the cosensitizer.[10] The JA1+TTR2 based-device showed the PCE of 6.75%, and the JA2+TTR2 based-device showed the highest PCE of 8.98%. The V_{oc} values of the cosensitized DSSCs were both much larger than the corresponding individual DSSCs. It is mainly because the cosensitizer TTR2 can occupy the voids between the main dye molecules (Fig. 8). This can avoid the main dye aggregation and prevent the I_3^- of the electrolyte penetrating into the TiO_2 surface, so as to reduce the charge recombination and improve the V_{oc} of the devices.[10,28] Remarkably, we found that the J_{sc} (13.42 mA cm^{-2}) of JA1+TTR2 increased 1.32 mA cm^{-2} compared with the J_{sc} (12.10 mA cm^{-2}) of JA1, whereas the J_{sc} (17.75 mA cm^{-2}) of JA2+TTR2 increased 2.73 mA cm^{-2} compared with the J_{sc} (15.02 mA cm^{-2}) of JA2. In order to study the causes of the differences clearly, we measured the adsorption amounts of the dyes (Table 3). In the case of the DSSCs based on JA1 and JA2 cosensitized with TTR2, the amount of TTR2 was estimated to be 4.67×10^{-8} and 1.65×10^{-8} mol cm^{-2}, respectively. On the other hand, the amount of JA1 decreased to 4.63×10^{-8} mol cm^{-2}, and the amount of JA2 (6.77×10^{-8} mol cm^{-2}) was nearly unchanged. The results

clearly indicate that there is almost no competitive adsorption between the JA2 and TTR2, in contrast, there is a serious competitive adsorption between the JA1 and TTR2. As shown in Figure 7b, the IPCE values of JA2+TTR2 exceeded 70% from 415 to 480 nm, and attained 82.1% at 450 nm and 67.4% at 628 nm. In contrast, the values of JA1+TTR2 were much lower than that of JA2+TTR2 (especially in the low energy absorption region), the maximum value of JA1+TTR2 was only 61.6% at 450 nm. The reduced amount of the dye JA1 adsorption was the main reason for the lower IPCE values of the JA1+TTR2 based-device. In order to further verify the results, we measured the UV-Vis absorption spectra of JA1+TTR2 and JA2+TTR2 adsorbed onto 14 μm thick TiO_2 substrate (Fig. 9). It is clear that the weak absorption of JA2 in the 460-600 nm range was compensated well by the dye TTR2. In contrast, although the weak absorption of JA1 in the 460-600 nm region was also compensated by the dye TTR2, but the absorption intensity of JA1 in the 400-460 nm region and the 600-660 nm region were both decreased. The result is consistent with the IPCE of the cosensitized DSSCs.

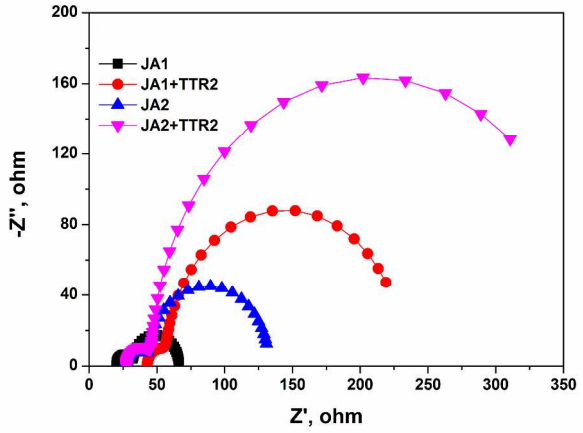

Fig. 10 Nyquist plots obtained in the dark of the DSSCs based on **JA1**, **JA2**, **JA1+TTR2** and **JA2+TTR2**.

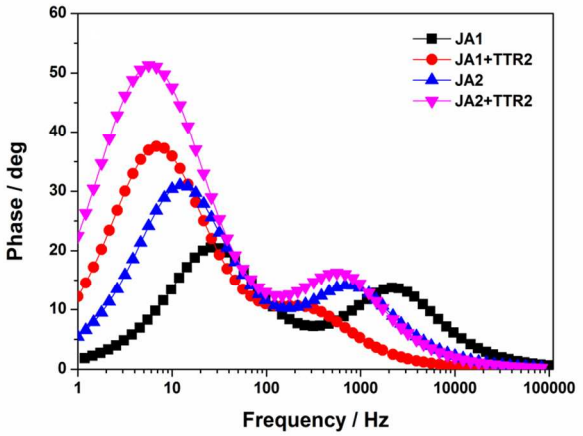

Fig. 11 Bode phase plots obtained in the dark of the DSSCs based on **JA1**, **JA2**, **JA1+TTR2** and **JA2+TTR2**.

Electrochemical Impedance Spectroscopy (EIS)

The Electrochemical Impedance Spectroscopy was measured under dark to further investigate the interfacial charge transfer process in DSSCs. The applied voltage was -0.7 V and scanned from 10^5 to 1 Hz. The Nyquist plots were shown in Fig. 10, and two semicircles were observed. For the Nyquist plots, the larger semicircle represents the charge recombination resistance (R_{rec}) at the TiO_2/dye/electrolyte interface, and the smaller semicircle represents the electron transport resistance at the Pt/electrolyte interface. It is clear that the radius of the larger semicircle decreased in the order JA2+TTR2 > JA1+TTR2 > JA2 > JA1, indicating that the JA2+TTR2 based-device has the largest R_{rec}. The device with large R_{rec} can suppress the charge recombination and reduce the dark current, thereby improving the V_{oc} of the DSSCs. The result is in agreement with the V_{oc} of the DSSCs.[52] The Bode phase plots of the DSSCs were shown in Fig. 11. The maximum frequency (ω_{max}) of the DSSCs with JA1 and JA2 was 25.6 and 12.0 Hz, respectively, those of the DSSCs with JA1+TTR2 and JA2+TTR2 was greatly reduced to 6.7 and 5.5 Hz, respectively. Since the maximum frequency was inversely related to the electron lifetime, the lower frequency corresponds to the larger charge recombination resistance and longer electron lifetime.[53] We further measured the EIS under illumination condition to probe the charge collection rate in the devices (Fig. S5). The radii of the large semicircle increase in the following order: JA2+TTR2 < JA1+TTR2 < JA2 < JA1, which indicates that JA2+TTR2 based-device has the smallest charge transfer resistance. Low charge transfer resistance observed for the JA2+TTR2 based-device suggests better electron collection efficiency over the other devices. Thus, we took dye TTR2 as the cosenzitizer can reduce the charge recombination rate and improve the performance of the device.

3. Conclusions

In summary, we developed a novel anchoring group which can anchor dye onto the TiO_2 surface via tridentate mode. The anchoring group can make the dye choose the Lewis acid sites and Brønsted acid sites of the TiO_2 synchronously. The JA2 based-device showed a higher PCE of 7.20%, whereas the JA1 based-device showed a PCE of 5.76%. The absorption spectrum of JA2 was not only red-shifted compared with JA1, moreover, the JA2 had better charge transport properties and higher electron injection efficiency. In addition, we took dye TTR2 as the cosensitizer, which can make up for the poor absorption of zinc-porphyrin dye in the 470-550 nm range. The dye TTR2 occupied the voids between the main dye molecules, thus preventing the I_3^- of the electrolyte penetrating into the TiO_2 surface, thereby reducing the charge recombination rate. We found that there was almost no competitive adsorption between JA2 and TTR2, in contrast, cosensitization of JA1 and TTR2 would cause serious competitive adsorption. The JA1+TTR2 based-device showed the PCE of 6.75%, whereas the JA2+TTR2 based-device showed the highest PCE of 8.98%. These results indicate that the performance of the DSSCs can be improved by developing a more efficient anchoring group.

Acknowledgements

This work was supported by grants from the National Natural Science Foundation of China (Nos. 21371092; 21401107), National Basic Research Program of China (2010CB923303), Natural Science Foundation of Jiangsu Province, China (No.

BK20140986).

Notes and references

[a] State Key Laboratory of Coordination Chemistry, School of Chemistry and Chemical Engineering, Collaborative Innovation Center of Advanced Microstructures, Nanjing University, Nanjing 210093, P. R. China, E-mail: zhenghg@nju.edu.cn. Fax: 86-25-83314502.
[b]School of Chemical Engineering, Nanjing University of Science and Technology, Nanjing 210094, P. R. China, E-mail: xhju@mail.njust.edu.cn

† Electronic supplementary information (ESI) available: synthesis details and characterization data; Details for all physical characterizations. See DOI: 10.1039/b000000x/

1 B. O'Regan, M. Grätzel, *Nature*, 1991, **353**, 737.
2 A. Hagfeldt, G. Boschloo, L. Sun, L. Kloo and H. Pettersson, *Chem. Rev.*, 2010, **110**, 6595.
3 L. L. Li, E. W. G. Diau, Chem. *Soc. Rev.*, 2013, **42**, 291.
4 A. Yella, C. L. Mai, S. M. Zakeeruddin, S. N. Chang, C. H. Hsieh, C. Y. Yeh and M. Grätzel, *Angew. Chem. Int. Ed.*, 2014, **53**, 2973.
5 J. Luo, M. Xu, R. Li, K. W. Huang, C. Jiang, Q. Qi, W. Zeng, J. Zhang, C. Chi, P. Wang and J. Wu, *J. Am. Chem. Soc.*, 2014, **136**, 265.
6 J. Yang, P. Ganesan, J. Teuscher, T. Moehl, Y. J. Kim, C. Yi, P. Comte, K. Pei, T. W. Holcombe, M. K. Nazeeruddin, J. Hua, S. M. Zakeeruddin, H. Tian and M. Grätzel, *J. Am. Chem. Soc.*, 2014, **136**, 5722.
7 M. K. Nazeeruddin, A. Kay, I. Rodicio, R. Humpbry-Baker, E. Miiller, P. Liska, N. Vlachopoulos and M. Grätzel, *J. Am. Chem. Soc.*, 1993, **115**, 6382.
8 D. Kuang, C. Klein, S. Ito, J. E. Moser, R. Humphry-Baker, N. Evans, F. Duriaux, C. Grätzel, S. M. Zakeeruddin and M. Grätzel, *Adv. Mater.*, 2007, **19**, 1133.
9 Q. J. Yu, Y. H. Wang, Z. H. Yi, N. N. Zu, J. Zhang, M. Zhang and P. Wang, *Acs, Nano.*, 2010, **4**, 6032.
10 Y. Wang, B. Chen, W. Wu, X. Li, W. Zhu, H. Tian and Y. Xie, *Angew. Chem. Int. Ed.*, 2014, **53**, 10779.
11 T. Ripolles-Sanchis, B. C. Guo, H. P. Wu, T. Y. Pan, H. W. Lee, S. R. Raga, F. Fabregat-Santiago, J. Bisquert, C. Y. Yeh and E. W. G. Diau, *Chem. Commun.*, 2012, **48**, 4368.
12 H. He, A. Gurung, L. Si and A. G. Sykes, *Chem. Commun.*, 2012, **48**, 7619.
13 S. Mathew, A. Yella, P. Gao, R. Humphry-Baker, B. F. E. Curchod, N. Ashari-Astani, I. Tavernelli, U. Rothlisberger, M. K. Nazeeruddin and M. Grätzel, *Nature Chemistry*, 2014, **6**, 242.
14 A. Nayak, R. R. Knauf, K. Hanson, L. Alibabaei, J. J. Concepcion, D. L. Ashford, J. L. Dempsey and T. J. Meyer, *Chem. Sci.*, 2014, **5**, 3115.
15 Y. Ooyama, Y. Harima, *ChemPhysChem*, 2012, **13**, 4032.
16 S. H. Chou, C. H. Tsai, C. C. Wu, D. Kumar and K. T. Wong, *Chem. Eur. J*, 2014, **20**, 16574.
17 Z. S. Wang, Y. Cui, K. Hara, Y. Dan-oh, C. Kasada and A. Shinpo, *Adv. Mater.*, 2007, **19**, 1138.
18 A. Baheti, K. R. J. Thomas, C. P. Lee, C. T. Li and K. C. Ho, *J. Mater. Chem. A*, 2014, **2**, 5766.
19 M. Cheng, X. Yang, C. Chen, J. Zhao, Q. Tian and L. Sun, *Phys. Chem. Chem. Phys.*, 2013, **15**, 17452.
20 H. Li, Y. Wu, Z. Geng, J. Liu, D. Xu and W. Zhu, *J. Mater. Chem. A*, 2014, **2**, 14649.
21 B. G. Kim, K. Chung, J. Kim, *Chem. Eur. J*, 2013, **19**, 5220.
22 Y. Ooyama, S. Inoue, T. Nagano, K. Kushimoto, J. Ohshita, I. Imae, K. Komaguchi and Y. Harima, *Angew. Chem. Int. Ed.*, 2011, **50**, 7429.
23 D. G. Brown, P. A. Schauer, J. Borau-Garcia, B. R. Fancy and C. P. Berlinguette, *J. Am. Chem. Soc.*, 2013, **135**, 1692.
24 W. Li, L. G. C. Rego, F. Q. Bai, J. Wang, R. Jia, L. M. Xie and H. X. Zhang, *J. Phys. Chem. Lett.*, 2014, **5**, 3992.
25 T. P. Brewster, S. J. Konezny, S. W. Sheehan, L. A. Martini, C. A. Schmuttenmaer, V. S. Batista and R. H. Crabtree, *Inorg. Chem.*, 2013, **52**, 6752.
26 F. Ambrosio, N. Martsinovich and A. Troisi, *J. Phys. Chem. Lett.*, 2012, **3**, 1531.
27 L. Martin-Gomis, F. Fernandez-Lazaro and A. Sastre-Santos, *J. Mater. Chem. A*, 2014, **2**, 15672.
28 N. Shibayama, H. Ozawa, M. Abe, Y. Ooyama and H. Arakawa, *Chem. Commun.*, 2014, **50**, 6398.
29 H. Kusama, T. Funaki, N. Koumura and K. Sayama, *Phys. Chem. Chem. Phys.*, 2014, **16**, 16166.
30 X. Lu, T. Lan, Z. Qin, Z.-S. Wang and G. Zhou, *ACS Appl. Mater. Interfaces.*, 2014, **6**, 19308.
31 X. Sun, Y. Wang, X. Li, H. Agren, W. Zhu, H. Tian and Y. Xie, *Chem. Commun.*, 2014, **50**, 15609.
32 G. Li, M. Liang, H. Wang, Z. Sun, L. Wang, Z. Wang and S. Xue, *Chem. Mater.*, 2013, **25**, 1713.
33 A. Yella, H. W. Lee, H. N. Tsao, C. Yi, A. K. Chandiran, M. K. Nazeeruddin, E. W. G. Diau, C. Y. Yeh, S. M. Zakeeruddin and M. Grätzel, *Science*, 2011, **334**, 629.
34 F. Gou, X. Jiang, B. Li, H. Jing and Z. Zhu, *ACS Appl. Mater. Interfaces.*, 2013, **5**, 12631.
35 T. Higashino, H. Imahori, *Dalton Trans*, 2015, **44**, 448.
36 M.-E. Ragoussi, T. Torres, *Chem. Commun.*, 2015, **51**, 3957.
37 M. Urbani, M. Gratzel, M. K. Nazeeruddin and T. Torres, *Chem. Rev.*, 2014, **114**, 12330.
38 C.-L. Wang, J-W. Shiu, Y.-N. Hsiao, P.-S. Chao, E. W.-G. Diau and C.-Y. Lin, *J. Phys. Chem. C*, 2014, **118**, 27801.
39 W. I. Hung, Y. Y. Liao, T. H. Lee, Y. C. Ting, J. S. Ni, W. S. Kao, J. T. Lin, T. C. Wei and Y. S. Yen, *Chem. Commun.*, 2015, **51**, 2152.
40 W. H. Nguyen, C. D. Bailie, J. Burschka, T. Moehl, M. Gratzel, M. D. McGehee and A. Sellinger, *Chem. Mater.*, 2013, **25**, 1519.
41 Y. Cui, Y. Wu, X. Lu, X. Zhang, G. Zhou, F. B. Miapeh, W. Zhu and Z. S. Wang, *Chem. Mater.*, 2011, **23**, 4394.
42 Z. M. Ju, H. L. Jia, X. H. Ju, X. F. Zhou, Z. Q. Shi, H. G. Zheng and M. D. Zhang, *RSC Adv*, 2015, **5**, 3720.
43 G. D. Sharma, S. P. Singh, R. Kurchaniac and R. J. Ball, *RSC Adv*, 2013, **3**, 6036.
44 H. L. Jia, Z. M. Ju, H. X. Sun, X. H. Ju, M. D. Zhang, X. F. Zhou and H, G. Zheng, *J. Mater. Chem. A*, 2014, **2**, 20841.
45 T. Hamamura, J. T. Dy, K. Tamaki, J. Nakazaki, S. Uchida, T. Kubo and H. Segawa, *Phys. Chem. Chem. Phys.*, 2014, **16**, 4551.
46 L.-Y. Lin, C.-H. Tsai, K.-T. Wong, T.-W. Huang, L. Hsieh, S.-H. Liu, H.-W. Lin, C.-C. Wu, S.-H. Chou, S.-H. Chen and A.-I. Tsai, *J. Org. Chem.*, 2010, **75**, 4778.
47 C.-H. Wu, M.-C. Chen, P.-C. Su, H.-H. Kuo, C.-L. Wang, C.-Y. Lu, C.-H. Tsai, C.-C. Wu and C.-Y. Lin, *J. Mater. Chem. A*, 2014, **2**, 991.
48 K. Chaitanya, X. H. Ju and B. M. Heron, *RSC Adv*, 2014, **4**, 26621.
49 L. Zhang, J. M. Cole, *ACS Appl. Mater. Interfaces.*, 2015, **7**, 3427.
50 Y. Ooyama, K. Uenaka, T. Sato, N. Shibayama and J. Ohshita, *RSC Adv*, 2015, **5**, 2531.
51 D. Barpuzary, A. S. Patra, J. V. Vaghasiya, B. G. Solanki, S. S. Soni and M. Quresh, *ACS Appl. Mater. Interfaces.*, 2014, **6**, 12629.
52 D. Kumar, K. R. J. Thomas, C.-P. Lee and K.-C. Ho, *J. Org. Chem.*, 2014, **79**, 3159.
53 S. H. Kang, I. T. Choi, M. S. Kang, Y. K. Eom, M. J. Ju, J. Y. Hong, H. S. Kang and H. K. Kim, *J. Mater. Chem. A*, 2013, **1**, 3977.